Scholar Publishing Group
International Journal of Big Data Intelligent Technology
https://doi.org/10.38007/IJBDIT.2020.010105
ISSN 2790-0932 Vol. 1, Issue 1: 73-89

Intelligent High-Speed Photovoltaic Road Signal Lamp Based on Intelligent Control of Nano-Composite Ceramic Substrate

Rashar Almajede*

American University in the Emirates, UAE

**corresponding author*

Keywords: Nanocomposite Ceramic Substrate, Intelligent Control, Intelligent High Speed, Road Signal Light

Abstract: At present, the metal substrate manufacturers in the world have developed a variety of different types of metal substrates. Metal substrates have now become the mainstream varieties of heat dissipation substrates for signal lamps. This research mainly discusses intelligent high-speed photovoltaic road signal lights based on intelligently controlled nano-composite ceramic substrates. The electroless copper plating method is used to densify the metalized AlN ceramic packaging substrate, and the metallization layer of the AlN ceramic packaging substrate by electroless copper plating is studied when a single complexing agent and a composite complexing agent are added to the electroless plating solution. And its performance impact. At room temperature, a laser is used to quickly scan the aluminum nitride ceramic substrate coated with a metal tungsten layer to achieve ceramic metallization and a firm connection between the ceramic and the metal. The surface, interface macroscopic and microscopic morphology, material composition and phase composition of the prepared W/AlN ceramic substrate were systematically analyzed, and the thermal conductivity and bonding strength of the metalized substrate were tested. The laser and the material were used. The nature of the interaction studies a new method of AlN ceramic metallization. The reasons for the junction temperature of photovoltaic road signal lamps and several common methods and physical mechanisms for measuring the junction temperature of semiconductor devices are reviewed. The forward voltage method is used to measure the voltage-temperature coefficient of high-power photovoltaic road signal lamps on AlN heat sink substrates with different metal transition layers. Tested with junction temperature, and finally discussed the influence of different metal transition layers on the heat dissipation performance of AlN heat sink substrate. When the sintering temperature reaches 1150℃, the bonding strength reaches the highest 9.7kg/mm2, and when the sintering temperature exceeds 1150℃, the bonding strength begins to decrease again. This research will effectively improve the reliability and lifespan of high-power smart high-speed photovoltaic road signal lights.

1. Introduction

Aluminum nitride has high thermal conductivity and is suitable for high-power, high-lead and large-size chips: its thermal expansion coefficient matches silicon, and its dielectric constant is low; its material has high mechanical strength and can still be used under severe conditions. Work as usual, so aluminum nitride ceramics can be made into the required substrate to meet the application requirements of different package substrates.

AlN ceramic has excellent properties such as high thermal conductivity, high strength, high resistivity, low density, low dielectric constant, non-toxicity, and thermal expansion coefficient matching silicon. It will gradually replace traditional high-power substrate materials and become the most A promising ceramic substrate material.

At present, the main problem of using air pressure sintering to prepare AlN ceramics with high thermal conductivity is that the thermal conductivity can be improved through long-time sintering and heat treatment, which leads to a sharp decline in the mechanical properties of materials and higher energy consumption. Kun Y combined multi-walled carbon nanotubes (MWNT) into a precursor derived ceramic made from polysilazane. Carbon nanotubes (CNT) reinforced ceramic nanocomposites of approximately 35 vol% are fabricated by permeating CNT preforms with liquid phase polymerization precursors and then pyrolysis. The indentation hardness of nano-composites without microcracks is lower than that of non-reinforced ceramics, but the results of microindentation test show that nano-composites have higher fracture energy. He believes that the influence of carbon nanotubes on the mechanical properties of nanocomposites should be discussed accordingly [1]. Darabi R R suggested that tfN-FO membranes were developed using polyethersulfone - ferrous oxide (PES-Fe_3O_4) nanocomposite substrates. After adding fe3o4 nanoparticles (NPs), the porosity and hydrophilicity of PES substrate are improved, the structural parameters (S value or S) are reduced, and the water flux is enhanced. To fabricate TFN films for FO applications, he produced thin polyamide layers by interfacing polymerization of m-phenylenediamine (MPD) and 1, 3, 5-benzoyl chloride (TMC) on the top surface of PES-Fe_3O_4 nanocomposite substrates. TFN membranes prepared with 0.2wt % PES-Fe $_3O_4$NPs showed the most reliable results by showing high water flux and low reverse solute flux. In addition, when 10 mm NaCl and seawater were used as feeding solution and 0.5 or 2 mL NaCl, TFN0.2 membrane showed a higher pure water flux in both Al-Fs and Al-DS directions than the control film composite (TFC) membrane as absorption solution [2]. Razzaghi M introduced a polymer/ceramic coating on magnesium based nanocomposites and evaluated the implant applications of nanocomposites. The microstructure, corrosion and biological activity of coated and uncoated samples were evaluated. $Mg_3Zn_{0.5}Ag_{15}$niti nanocomposite substrate was fabricated by mechanical alloying and sintering. In addition, he looked at different amounts of poly (lactic acid-glycolic acid copolymer) (PLGA) coatings and chose a PLGA content of 10wt%. Electron microscope (SEM) images show acceptable uniform dispersion of NiTi nanoparticles (NPs) in Mg matrix. The Ca/P atomic ratio indicates that the amount of apatite formation on the coated sample is greater than that on the uncoated nanocomposite [3]. Ceramic polymer composites with high dielectric constant have been produced by heat treatment in the range of 160 to 200℃. Kim S W introduced a room-temperature process for generating flexible high dielectric constant nanocomposite films on polymer substrates by combining printing technology with UV curing process. The composite structure is based on nanoscale BaTiO3 and Ag particles dispersed in a uV-cured polymer matrix. The dielectric properties of the thick nanocomposite films depend on the volume fraction and particle size of $BaTiO_3$ and the content of Ag. As a best result, a dielectric constant of ~300 and a dielectric loss of

0.08 were achieved when 81 nm $BaTiO_3$ and 34 nm Ag particles were used at 56.2% overall integrals, which is very competitive for flexible capacitor devices. The current-voltage behavior of nanocomposite films largely depends on the Ag content associated with conductive osmotic transition [4]. Nanocomposite thick film electrodes have been investigated for use in highly integrated microcircuit devices requiring delayed densification to match potential co-fired ceramic sheets. Jin W J introduced carbon nanotubes (CNT) as a component to prevent densification of the conductive nickel paste and minimize the reduction of the resistivity of the paste. A well-dispersed CNT/Ni paste containing 1 to 5wt% of various quantities of CNT was screen-printed on an ordinary alumina substrate and fired in a reducing atmosphere at 800-1200℃ for 1 hour. The delay effect is significant even when complete densification is shown at 1100℃ using 1wt% CNT, which corresponds to the target firing temperature of ceramic flakes. The resistivity is not significantly affected by the low CNT content, which corresponds to 3.39×10^5 ω /cm compared with 2.97×10 5 ω /cm of pure Ni paste treated at 1100℃ [5]. Fathian Z considers SN-0.7Cu to be one of the cheapest lead-free solder types available. However, its poor mechanical properties limit its application. He synthesized Sn-Cu lead-free solder reinforced with amorphous silica nanoparticles through the POWDER metallurgy route. The required mixture of raw materials is mechanically ground, compressed, sintered and extruded to prepare a large number of solder samples. He characterized the samples through optical and electron microscopes and mechanical tests. He improved the mechanical properties by adding nanoparticles to the solder matrix. The tensile strength, yield strength and compressive strength increased by 27%, 23% and 41%, respectively, after adding 1.5wt % ceramic reinforcement to the composite compared with the whole sample. In addition, ceramic nanoparticles reduced the wettability angle between the substrate and nanocomposite solder by 50%[6]. Blinov I presents experimental results of magnetic properties, resistivity and magnetic resistance (MR), with emphasis on $(Co_{40}Fe_{40}B_{20})_{(x)}(SiO_2)_{(100-x)}$ and $(Co_{84}Nb_{14}Ta_2)_{(x)}(Al_2O_3)_{(100-X)}$ nanocomposites close to the permeability threshold. X = 47-58 at.% nanocomposite films were deposited on glass ceramic substrates by ion beam sputtering. The sample consists of metal nanoparticles embedded in a non-stoichiometric matrix. Based on the structure and magnetic data, a large number of metal atoms are dispersed among the magnetic nanoparticles. As the metal volume fraction decreases, the temperature dependence of conductivity changes from InT behavior change, strong tunnel coupling between matching nanoparticles, to t-1/2 dependence below the metal-insulator transition. MR is studied in a pulsed magnetic field up to 20 T at T = 65-300 K. The pulse duration was 11 ms. Negative MR almost saturates with increasing magnetic field, but slowly increases or decreases in high magnetic field [7]. At present the application of road lamp power is increased, the chip in the accumulation of a lot of calories needed to be lost in time, if the brazing joint technology was applied to high power road lamp encapsulation structure, is bound to promote power road lamp encapsulation structure of heat dissipation ability, for the high power road lights, heat dissipation problems provides an effective solution.

AlN ceramic substrates can be used to package high-power devices for effective heat dissipation due to their high thermal conductivity, high temperature corrosion resistance, high temperature stability, high strength and hardness, and will have a wide range of application prospects in the field of electronic packaging. Using metal W as the metal coating material, using a laser that generates a Gaussian beam to quickly scan the aluminum nitride ceramic metallization, the refractory metal tungsten powder is instantly melted on the AlN ceramic sheet, and the two are quickly connected, which can be used for aluminum nitride at room temperature. The ceramic surface is quickly metallized to achieve a firm connection between AlN ceramic metal and tungsten.

2. Research Plan for Smart High-Speed Photovoltaic Pavement Signal Lights Based on Nanocomposite Ceramic Substrates

2.1. Selection of Ceramic Substrate Materials

Some physical properties of several common ceramic substrate materials are shown in Table 1.

Table 1. Some physical properties of several common ceramic substrate materials

Material properties	Al_2O_3	AlN	BN	BeO	Si
Dielectric constant	8.5-10	8.5-10	4	6.5-8.9	12
Resistivity (Ω/cm)	$> 10^4$	$> 10^{14}$	$> 10^{14}$	$>10^{14}$	$> 10^5$
Coefficient of thermal expansion (ppm/K)	6.5-7.2	2.7-4.6	4.1	6.3-9.0	2.6
Thermal conductivity (W/mrK)	22-40	100-260	33	260-300	20-150
Density (kg/cm3)	3.75-4.0	3.2	2.27	2.95	233
Flexural strength (MPa)	300-385	280-320	170	170-240	690

It can be seen from Table 1 that the thermal conductivity and thermal expansion coefficient of Al_2O_3 ceramics are low, and the heat dissipation capacity for high-power devices is not good; BeO powder is highly toxic and has high production costs, which limits its promotion and application; the production process of SiC ceramic materials is still Immature, and its dielectric constant is relatively high; AlN ceramic substrate material is compatible with Si, GaAs and other semiconductor materials due to its thermal expansion coefficient, and its performance is superior to Al_2O_3 and BeO, and there is no toxicity problem. Therefore, it has a wider range of applications, but At this stage, its manufacturing technology and process are not mature enough, and its high manufacturing cost is its shortcomings. In summary, AlN ceramic substrate has excellent thermal conductivity, insulation and other properties. It is an ideal new-generation packaging substrate material. It has broad application prospects in the electronics industry. The research and development of AlN substrate materials, therefore, in this paper, AlN ceramic is selected as the substrate material for high-power LED heat dissipation to carry out related application research.

Although AlN ceramics have many advantages such as high thermal conductivity and low thermal expansion coefficient, the complex preparation process of core raw material AlN powder, high price and high energy consumption limit the development of AlN ceramics. AlN powder basically relies on imports, and the instability of raw material batches and high preparation costs have become the bottleneck for the preparation of high-end AlN ceramic substrate materials. In addition, AlN ceramics have low strength, poor toughness, and easy to deliquesce. It is difficult to guarantee the due service life in a complex environment, and it damages semiconductor devices and increases the cost of use.

The experimental materials prepared by AlN metallized ceramic packaging substrates for high-power road signal lamps are shown in Table 2.

Table 2. Experimental materials prepared by AlN metallized ceramic packaging substrates for high-power road signal lights

Reagent name	Specification	Manufacturer
Aluminum nitride ceramics	99.5%	Fujian Huaqing Electronic Materials Co., Ltd.
Copper powder	99.6%	Sinopharm Chemical Reagent
Castor oil	CP	Guangdong Guanghua Chemical Factory
Polyethylene glycol	AR	Sinopharm Chemical Reagent
Phthalates	200cPaS	Sinopharm Chemical Reagent
Ethyl cellulose	CP	Sinopharm Chemical Reagent

2.2. Electroless Plating

Electroless plating refers to the use of a reducing agent to reduce and deposit the metal copper ions in the solution on the surface of the catalytically active AlN ceramic substrate to form a metal copper coating under the condition of no applied current. In the metallized ceramic substrate prepared by electroless plating, the interface between the AlN and the copper layer is mainly mechanically locked, and the bonding strength largely depends on the roughness of the ceramic substrate surface. The higher the intensity. In summary, the electroless plating process is simple, and the bonding strength between the ceramic substrate surface and the coating metal obtained by this method is high, which is suitable for mass production. In this paper, the electroless copper plating method is used to metalize the AlN ceramic substrate surface.

2.3. Selection of Electroless Copper Plating Bath Factors

(1) Complexing agent

The selected reducing agent formaldehyde has the reducing ability only in a strong alkaline environment with a pH greater than 7, so a complexing agent that can reduce the free Cu in the plating solution and prevent $Cu(OH)_2$ precipitation must be added to the plating solution. Commonly used complexing agents are tartaric acid, potassium sodium tartrate, ethylenediaminetetraacetic acid (EDTA) and so on. Tartaric acid is often used in room temperature and low deposition rate plating solutions; when EDTA is used as a complexing agent, the plating solution has good stability, fast plating speed, and good coating quality, but the temperature required for the chemical plating solution is high and the price is relatively expensive. Therefore, consider potassium and sodium tartrate can produce electroless copper plating reaction at low temperature, and the cost is low. In this experiment, potassium sodium tartrate was used as the complexing agent for electroless copper plating on the surface of AlN ceramic substrate.

(2) PH value regulator

In this test, formaldehyde has reducibility only in strong alkaline solutions. Therefore, strong alkaline reagents must be used to adjust the pH of the plating solution. In this test, sodium hydroxide solution is used as the pH regulator.

(3) Buffer and other ingredients

Hydrogen ions are generated during the electroless copper plating reaction, which reduces the pH of the plating solution. Therefore, sodium carbonate is selected as the pH buffer of the plating solution in this experiment; and the plating solution is added to the plating solution to accelerate the reaction of the plating solution and smooth the plating layer.

AlN ceramic substrates are non-metallic materials with low chemical activity and are difficult to plate substrates. Therefore, the surface of the substrate must be pre-treated before electroless copper plating. The pre-processing process is shown in Figure 1.

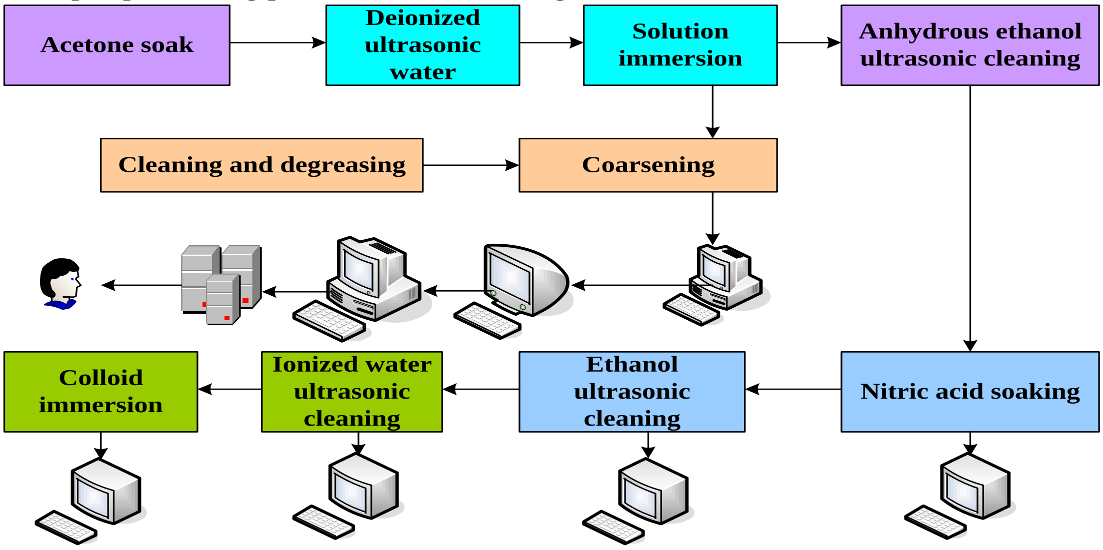

Figure 1. Pre-processing process

2.4. Preparation of AlN Metallized Ceramic Substrate

The ceramic substrate used in the experiment is an AlN ceramic sheet provided by Huaqing Electronic Materials Co., Ltd., with a thickness of 0.68mm and a size of 18×18mm.

(1) Ingredients

The experimental raw materials are mainly composed of AlN ceramic substrate and Cu-based compound slurry, and the mixing ratio of metal oxide is 1-10wt%. The components of the Cu-based compound slurry are shown in Table 3.

Table 3. Components of Cu-based compound slurry

Composition	Effect	Mass/g
CuO (M_xO_y)	Functional phase	20
castor oil	Thixotropic Agent	0.15
Dibutyl phthalate (DBP)	Solvent	0.1
Polyethylene glycol (PEG)	Wetting agent	0.15
Ethyl cellulose (5%)	Thickener	0.175
Terpineol (95%)	Solvent	3.325

(2) Coating process

The AlN substrate was first placed in acetone for ultrasonic cleaning for 15 minutes, and then rinsed with distilled water after being taken out, and finally placed in an oven to dry for later use. The thick film paste was coated on the AlN substrate by a screen printing process, and then placed in an electric heating constant temperature blast drying oven at 60℃ to dry for 1 hour.

(3) Screen printing process

Take 96 alumina ceramic sheets, polish them with sandpaper, put them into ethanol solution, and ultrasonically clean them in an ultrasonic cleaner for 30 minutes, and then print the prepared slurry on the alumina ceramics through a metal screen surface. If the screen sticks to the substrate or leaves a large amount of paste in the mesh during printing, and the disconnection occurs at the specified printing speed, it is considered that the printability of the paste is not good: if the screen leaves the substrate smoothly after printing, moreover, there is little paste left in the mesh, and the required resolution is obtained at the same time. At this time, it is considered that the printability of the paste is good. Based on the above measurement standards, this paper has formulated a cuprous oxide electronic paste with relatively good leveling and high precision.

(4) Sintering process

Put the dried AlN ceramic substrate into a high-temperature furnace and slowly heat it to 1000~1100℃ at a heating rate of 10℃/min, and keep it for 30min, and then cool it with the furnace. The whole process is carried out under air conditions. The purpose of sintering mainly includes two points: 1) remove the organic components in the thick film slurry; 2) make the thick film slurry react with AlN at high temperature to form an intermediate phase, and realize the connection between the surface film layer and the ceramic substrate.

The critical shear stress required for the unit area film to peel from the substrate[8-9]:

$$f = \left[w/\left(\pi R^2 - W\right)\right] * P \tag{1}$$

R is the radius of curvature of the needle tip; P is the reaction force of the substrate at the point L. The P value can be obtained by measuring the indentation width d[10]:

$$d = 2a = \Re\left[W / \pi P\right] \tag{2}$$

The temperature caused by the interface can be expressed as[11]:

$$\Delta T = \Delta T_C + M\Delta T_C \tag{3}$$

You can get[12]:

$$\frac{\Delta T}{Q} = \frac{\Delta \mathrm{x}}{\lambda} + \frac{m}{n} \tag{4}$$

(5) Reduction process

1) Hydrogen reduction process

After sintering, the Al_2O_3 ceramic package substrate is reduced in a hydrogen reducing medium, and the reducing atmosphere is hydrogen and nitrogen.

A mixed gas with a volume ratio of 1:2. The reduction reaction started at 600℃, and the reduction reaction proceeded completely at 900℃, and a metalized Cu layer was formed on the surface of the substrate, which was then cooled down to room temperature with the furnace.

2) Carbon reduction process

The sintered AlN ceramic package substrate is reduced in the carbon powder reduction medium. When reducing, first put the substrate flat in an alumina crucible, and then cover a layer of carbon powder with a thickness of about 5mm on the substrate, and finally reduce it in a vacuum pit furnace while passing in a certain amount of nitrogen protective gas. After reduction at 800℃ and 850℃, the surface of the substrate did not change significantly and remained black; after reduction at 900℃, the surface of the substrate changed from black to dark red; and after reduction at 950℃, 1000℃, 1050℃, and 1075℃, the surface of the substrate became it is pale pink. From the surface color change of the sintered substrate, it can be preliminarily inferred that the carbon reduction reaction can proceed completely when the reduction temperature reaches above 950℃. In order to obtain all the metallic Cu layers, the reduction temperature should be above 950℃.

2.5. Characterization and Detection of Samples

(1) Surface topography

A scanning electron microscope (SEM) was used to observe the surface morphology of the sample. Observation of the micro-morphology of the AlN ceramic package substrate the experimental sample was used for the observation of the micro-morphology using Hitachi's SU8010 field emission scanning electron microscope for scanning observation, with an acceleration voltage of 20kV. Before the sample is scanned, it must be fixed on the standard sample table with conductive adhesive or double-sided adhesive, and then gold-plated on the surface for 60 seconds under vacuum conditions.

(2) Coating composition

An energy spectrometer (EDS) was used to detect the composition of the AlN ceramic substrate and its coating.

(3) Plating structure

X-ray diffractometer (XRD) was used to analyze the structure of the coating.

(4) Deposition rate

Use the weighing method to calculate the deposition rate of the coating. The deposition rate v of electroless copper plating on the surface of AlN ceramic substrate using this process can be expressed as [13]:

$$v = \frac{M_2 - M_1}{t * a^2} \tag{5}$$

(5) Coating adhesion

Use the scratch test to judge the quality of the combination of the copper coating and the AlN ceramic substrate surface;

(6) Conductivity

Use the Hall detector HMS-5000 to detect the conductivity of the copper coating;

(7) Surface resistivity test

1) Choose a suitable electrode material, which should be a kind of conductive material that is easy to add to the sample, can be in close contact with the sample surface, and will not introduce large errors due to electrode resistance or contamination of the sample.

2) It is very important that the stray current between the electrodes or between the measuring electrode and the ground has no obvious influence on the reading of the test instrument. Be extremely careful when adding electrodes to the sample and placing the sample during the test, so as not to cause any discrepancies in the test results.

Good influence of stray current channels. When measuring surface resistance, do not clean the surface, except that the untouched surface of another sample of the same material can touch the tested sample, and the tested part of the surface should not be touched by anything.

3) The processing conditions of the sample are processed according to GB/T 10580-2003. Because the surface resistivity is particularly sensitive to temperature changes, this change is exponential, so the surface resistivity of the sample must be measured under the specified conditions.

(8) Thermal conductivity

The German NETZSCH LFA 457 Leading Thermal Analysis was used to measure the thermal conductivity of Al ceramic copper-plated substrates.

The factor level is coded according to the following formula [14-15]:

$$x = \frac{X_i - X}{\Delta X} \tag{6}$$

Among them, X_i is the coded value of the i-th factor [16].

The second-order model is used to optimize the response surface. The second-order model used is as follows [17]:

$$Y = \beta + \sum_{i=1}^{k} \beta x + \sum_{i=1}^{k} \beta_1 x_1 + \sum_{i=1}^{k} \beta_2 x_2 + \sum_{i=1}^{k} \beta_1 x_m x_n \tag{7}$$

Among them, x is the input variable, that is, the code value of the i-th factor, which affects the response variable Y.

(9) Porosity test

When observing the microscopic morphology of the metallization layer of the ceramic package substrate, in order to quantitatively express the density of the metallization layer, the experiment uses the porosity as the evaluation index. The porosity measurement method is to use ImageTools image processing software to analyze the black and white degree of the SEM picture, and then ImageTools software calculates the porosity of the metalized layer surface according to the proportion of the black and white degree in the picture.

In the process of material preparation and synthesis, due to process conditions and other reasons, there are often pores or hole defects, resulting in material performance degradation. In order to measure the volume occupied by pores or holes in the material, it is usually expressed by the physical quantity of porosity. The porosity of a material specifically refers to the percentage of the volume of pores inside the material to the total volume of the material, denoted by *P*. The calculation formula is [18-19]:

$$P = \frac{V_0 - V}{V} \times 100\% \tag{8}$$

V is the absolute compact volume of the material, excluding pores.

3. Research Results of Nanocomposite Ceramic Substrates

Figure 2 shows the weight loss curve measured when the pure solvent is kept at different temperatures for 20 minutes and then cooled. In order to make the slurry not easy to volatilize at low temperature, but can quickly volatilize at the drying temperature, the method of mixed solvents can be used, and the volatilization characteristics of the organic carrier can be adjusted by changing the ratio.

At different sintering temperatures, the AlN interface phase composition (XRD) is shown in Figure 3. It can be seen from Figure 3 that when sintered at 800℃, no new phases were formed at the sample interface except the initial phase. When the sintering temperature was increased to 1150℃, $CuAlO_2$ and CuO phases appeared at the interface. According to the Cu_2O-AlN phase diagram, at a lower sintering temperature, there is no chemical reaction between the initial phase and Al_2O_3. When the temperature rises to 1000℃, Cu_2O is the stable phase, and the Cu_2O-AlN solid phase reaction line is reached at this time. The Cu_2O inside the layer reacts with alumina ceramics to produce $CuAlO_2$.

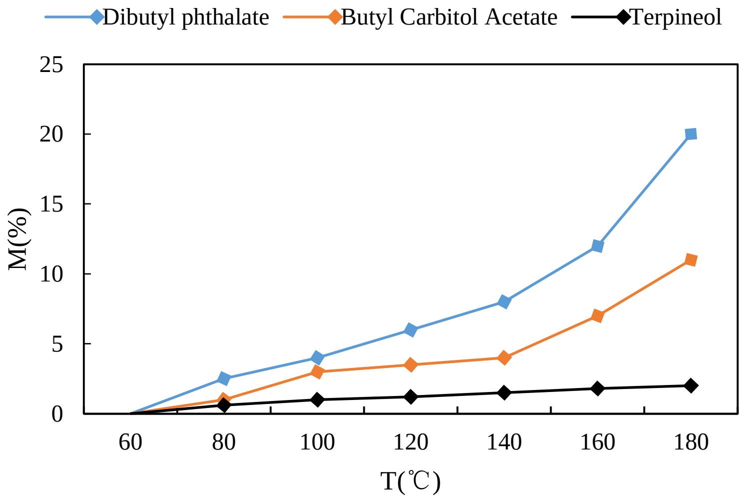

Figure 2. Weight loss curve measured when pure solvent is kept at different temperatures for 20 minutes and then cooled

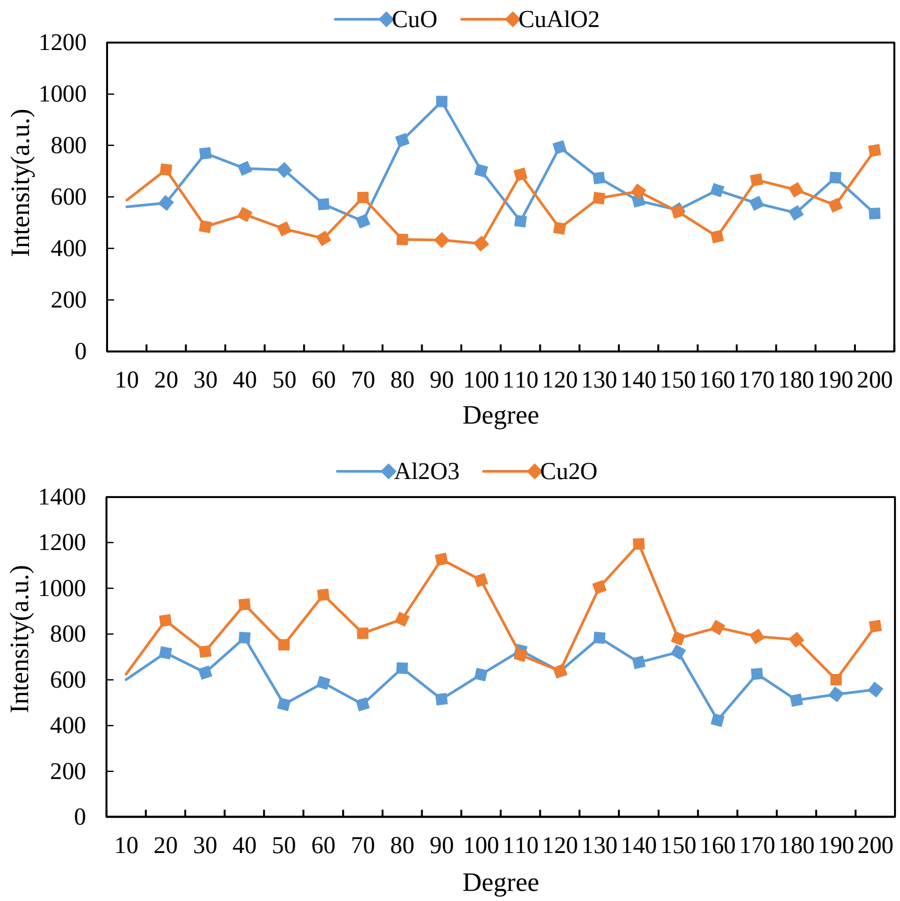

Figure 3. AlN interface phase composition (XRD) at different sintering temperatures

With the increase of the sintering temperature, the bonding strength of the substrate has also been continuously improved. When sintering at 800℃ and 900℃, the bonding strength is very low, about 1.0kg/mm^2. When the sintering temperature reaches 1150℃, the bonding strength reaches the highest 9.7kg/mm^2, and when the sintering temperature exceeds 1150℃, the bonding The intensity began to show a downward trend again. The change in the bonding strength of the substrate is shown in Figure 4.

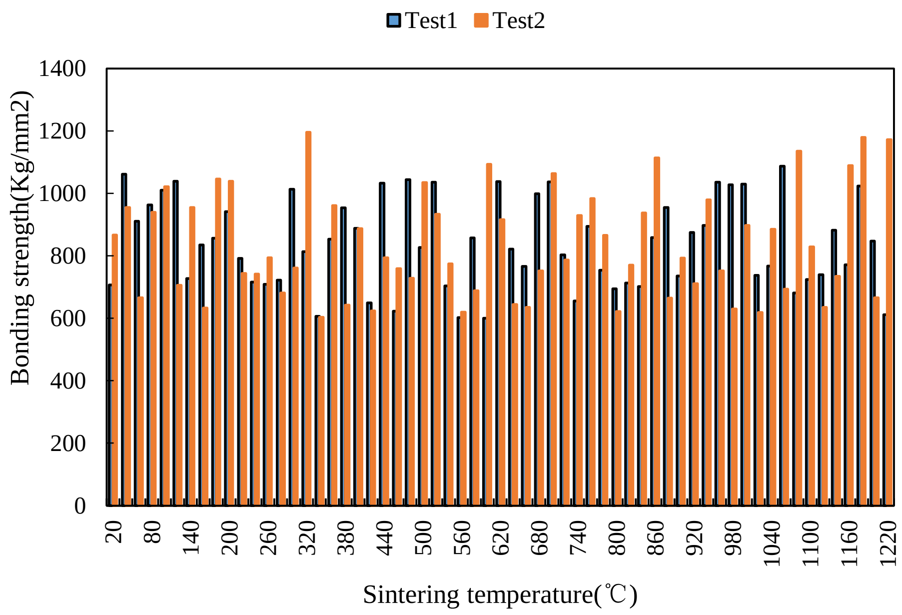

Figure 4. Change in bonding strength of substrate

The results of the substrate bonding strength in the orthogonal test and the range analysis are shown in Table 4.

Table 4. The results of the substrate bonding strength in the orthogonal test and the range analysis

Experiment number	Current density (A/dm^2)	Solution temperature (℃)	Time (min)
1	5	15	15
2	10	30	30
3	5	40	60
4	10	30	60
5	5	40	15

It can be seen from Figure 5 that as the current density increases, the substrate bonding strength is gradually increasing. However, when the current density exceeds 5A/dm^2, the increase rate of the bonding strength is slowed down; on the other hand, when the current density is too large, a large amount of Joule heat is generated, and the resulting film is easy to become loose or even fragile, and the metal matrix It is also prone to over-corrosion, so the current density should not be too large, and 5A/dm^2 is the best. The changes in current density and substrate bonding strength at different times are shown in Figure 5.

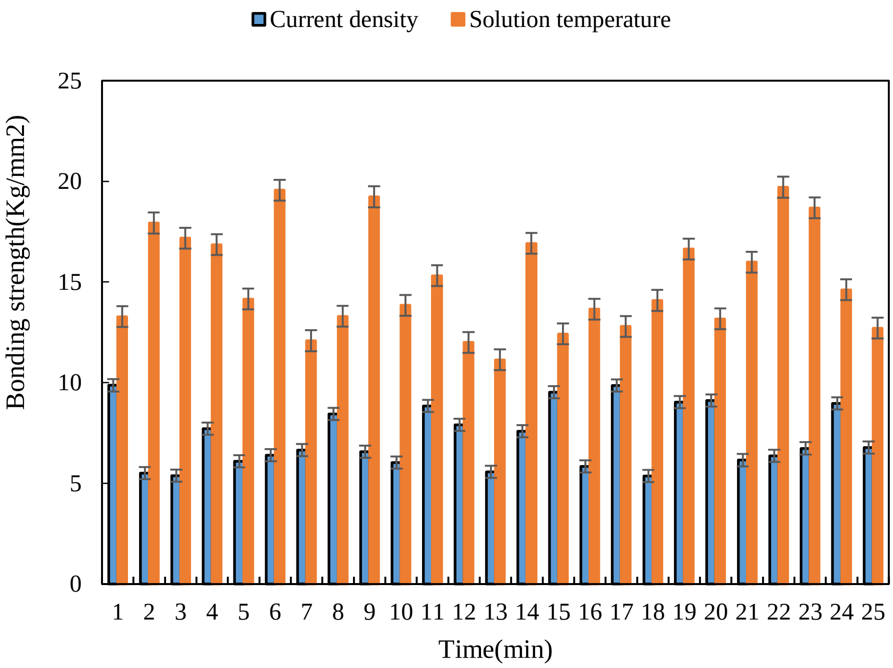

Figure 5. Changes in current density and substrate bonding strength at different times

The relationship curve between each test current and junction temperature drawn according to the voltage-temperature coefficient k of the signal lamp on each substrate is shown in Figure 6. It can be seen from Figure 6 that the junction temperature of the road signal lamp on the Cu/Ti/AlN substrate and the Cu/Al/Ti/AlN substrate increases with the increase of the test current, but on the Cu/Al/AlN substrate and the Cu/Al/AlN substrate. The junction temperature on the AlN substrate shows a tendency to increase first and then remain basically unchanged with the increase of the test current. This is all due to the fact that the road signal lamp generates more heat under larger test currents, and the thermal conductivity of metal Ti (n=17m·W/K) is higher than the thermal conductivity of the other three materials (Ahw=170m· W/K, h.=212m·W/K, h=255m·W/K) should be low, thereby hindering the heat conduction of the sample, resulting in the road signal lamp on the Cu/Ti/AlN substrate and Cu/A/Ti/AlN The junction temperature on the substrate continues to rise under a larger current, and the other two substrates have high thermal conductivity due to the absence of metal Ti, and the thermal conductivity of AlN, Al, and Cu are basically high under the larger test current. constant. At a small test current (100-200mA), the junction temperature of the road signal lamp on the AlN substrate with the transition layer is lower than the junction temperature on the AlN substrate without the transition layer; the junction temperature ratio on the AlN substrate with the multilayer transition layer the junction temperature on the single-layer transition layer AlN substrate should be low. This is attributed to the existence of the transition layer indirectly increasing the wettability of AlN ceramics and metallic Cu, reducing defects such as pores in the surface contact layer of AlN ceramics and metallic Cu, thereby improving the thermal conductivity of the entire sample.

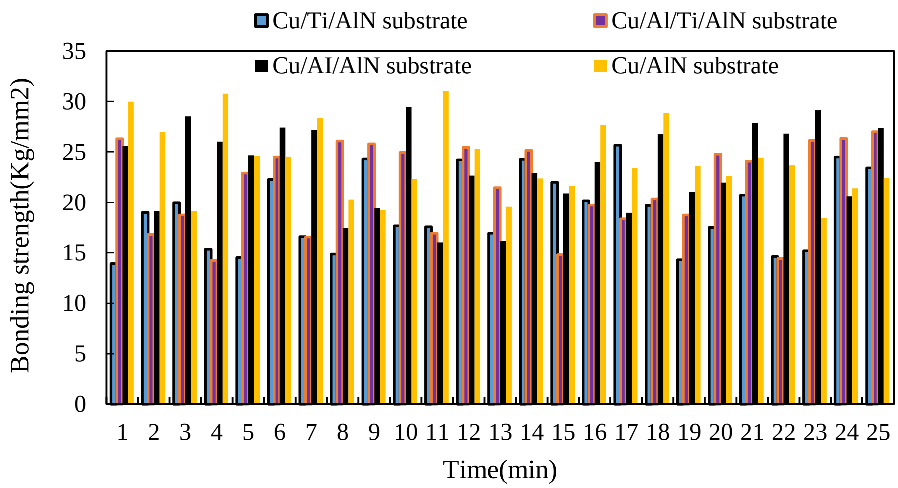

Figure 6. The relationship between each test current and junction temperature drawn based on the voltage-temperature coefficient k of the signal lamp on each substrate

4. Discussion

70%-80% of the energy in the high-power road signal lamp is converted into heat, and this heat has a serious impact on the performance of the road signal lamp, especially the impact on the life and light efficiency. Therefore, there is an urgent need for high-speed and effective heat dissipation technology to solve the problem. Heat management issues of power road signal lights. Due to its high thermal conductivity, high temperature corrosion resistance, high temperature stability, high strength and hardness, AlN ceramic substrates can be used to package high-power devices for effective heat dissipation, and will have a wide range of application prospects in the field of electronic packaging. However, the metallization of AlN ceramic substrates has problems such as low adhesion between the Cu coating and the substrate, and poor thermal stability of the Cu coating. Therefore, this study aims to address the above shortcomings and select the AlN ceramic substrate to prepare electroless Cu on its surface. And study the effect of annealing on the bonding force of the Cu coating, and package the AlN ceramic copper-plated substrate with the best performance with the road signal lamp to study the heat dissipation performance of this structure, and use the COMSOL Multiphysics software to evaluate the electrical heating performance of the road signal lamp after packaging simulation research hopes to provide guiding significance by studying the heat dissipation of AlN ceramic substrates in high-power road signal lamps and the application of finite element simulation software in scientific research [20].

At present, the wave of new technological revolution is in the ascendant, a series of high and new technology represented by information technology and microelectronics are developing rapidly, and the development of modern science and technology has increasingly higher requirements for the performance of various materials. The experiment compares the breakdown field strength of different samples and the results of the EDS test, and explores the influence of reaction power, target base distance, partial pressure ratio and air supply on the element content and breakdown field strength in the film, and seeks to improve the breakdown. The way to penetrate the field strength [21-22]. The Cu layer and the transition layer Ti and Al are tightly covered on the substrate. Even in the gap between the AlN grains, the metal layer and the substrate are well combined, which further shows that the use of vacuum evaporation coating and magnetron sputtering technology can achieve the metalization of the AlN ceramic substrate. The metal elements in each layer are in an independent distribution. However, there is also mutual diffusion of elements between the metal layer and the metal layer, which is conducive to the reaction between the metal and the metal to form intermetallic compounds, which improves the bonding strength between the metal layers, thereby improving the adhesion strength of the entire metal layer on the surface of the ceramic substrate [23].

Due to the advantages of energy saving, environmental protection, long life, small size, informationization, etc., the semiconductor lighting of road signal lamps has been used in various fields such as various indicators, backlight sources, general lighting and urban night scenes [24-25]. Nowadays, the global energy is in a state of shortage, so how to effectively use energy is an important issue facing us in the future. When the medium is very thin, the impact ionization has not been multiplied to the extent that it can destroy the film, and the electron avalanche has entered the anode recombination. At this time, the dielectric cannot be broken down, that is, the dielectric breakdown field strength will increase at this time. Even if the crystal quality is not ideal, AlN film coated with Al substrate may also be used in the packaging of multi-chip road signal lamps [26].

Air pressure sintering is the best process method for large-scale preparation of ceramic substrate materials. Compared with other sintering equipment, the large-scale pneumatic sintering furnace can prepare more substrate materials at one time, greatly reducing the preparation cost. Therefore, devoting to optimizing the air pressure sintering process to prepare high thermal conductivity AlN ceramics is of great significance to the industrialization of AlN ceramic substrates. With the gradual development of electronic components to high power, high density and high integration, a variety of new technologies and new structures have emerged in microelectronic packaging, such as wafer-level module packaging (WSP) and multi-chip packaging (MCP) Wait. These new packaging modes require low-temperature co-firing of packaging materials and circuit materials to achieve high-density and high-reliability packaging [27-28].

Since more low-melting components are generally added to the composition of ceramic substrates, a certain amount of liquid phase will appear during low-temperature sintering. As the temperature rises, the subsequent sintering process should be consistent with the glass/ceramic The second or third sintering mechanism of the system is consistent, which depends on the properties of other components. In the field of energy and transportation, semiconductor devices and high-power power electronic modules used on a large scale in industries such as wind power generation, solar photovoltaic power generation, electric vehicles, and high-speed rail are increasingly occupying an indispensable place, such as single-chip packaging or multi-chip packaging. The chips are cascaded and packaged into power conversion modules such as half-bridge and full-bridge, which provide power management for the power supply system or motor inverter system, and the power is very high. The packaged chip and the plating layer in the semiconductor are metal, both of which have good heat dissipation. The substrate material, which plays the role of bearing and insulation, is the key to the heat dissipation of the entire semiconductor device. On the basis of comprehensively summarizing existing related research results, according to the performance requirements of advanced electronic packaging for low-temperature co-fired ceramic substrate materials, impedance analyzer, thermal expansion coefficient tester, thermal conductivity tester, flexural strength tester, analysis and testing equipment, such as microhardness tester, systematically studied the influence of additives on ceramic structure, sintering performance, phase transition process, mechanical properties and so on. This research proposes a novel pavement signal lamp heat dissipation package structure and its preparation process that use metal aluminum as a substrate, plate aluminum nitride film on it as an insulating and thermally conductive layer, and then sputter a conductive layer on the

AlN film [29] .

5. Conclusion

In this study, the copper-based thick film electronic paste was used to study the metallization process of alumina ceramic packaging substrates. In order to improve the performance of the substrate, the substrate was densified by different methods. Finally, in view of the problem of large thermal resistance in the packaging structure of ordinary signal lights, based on the improved AlN ceramic packaging substrate, a new packaging structure in which the packaging substrate is soldered to the heat sink is proposed, which realizes the high-power signal lamp. Low thermal resistance package. The copper-based thick film electronic paste is spin-coated on the surface of alumina ceramics, and the metallization is performed through sintering and reduction processes. The formation mechanism of the metallization layer is studied. The performance of AlN ceramic package substrates is compared. In the research on the insulating properties of aluminum nitride films, limited to laboratory conditions and research time constraints, there is no further in-depth exploration. However, the practice of arc sputtering requires a large degree of change to the existing magnetron sputtering equipment. This method has not been studied in depth. If the subsequent experimental conditions are mature, further research can be done in this section.

Funding

This article is not supported by any foundation.

Data Availability

Data sharing is not applicable to this article as no new data were created or analysed in this study.

Conflict of Interest

The author states that this article has no conflict of interest.

References

[1] Kun Y , Laifei C , Linan A N , et al. Ceramic nanocomposites reinforced with a high volume fraction of carbon nanotubes. Journal of Wuhan University of Technology-Mater Sci Ed, 2017, 32(001):47-50. https://doi.org/10.1007/s11595-017-1556-3

[2] Darabi R R , Peyravi M , Jahanshahi M , et al. Decreasing ICP of forward osmosis (TFN-FO) membrane through modifying PES-Fe 3 O 4 nanocomposite substrate. Korean Journal of Chemical Engineering, 2017, 34(8):2311-2324. https://doi.org/10.1007/s11814-017-0086-1

[3] Razzaghi M , Kasiri-Asgarani M , Bakhsheshi-Rad H R , et al. In vitro bioactivity and corrosion of PLGA/hardystonite composite-coated magnesium-based nanocomposite for implant applications. International Journal of Minerals, Metallurgy and Materials, 2021, 28(1):168-178. https://doi.org/10.1007/s12613-020-2072-6

[4] Kim S W , Choi H R , Han C S , et al. Dielectric and current–voltage characteristics of flexible Ag/BaTiO 3 nanocomposite films processed at near room temperature. RSC Advances,

2017, 7(88):56038-56043. https://doi.org/10.1039/C7RA11640C
[5] Jin W J , Hong J C , Kwon O H , et al. Densification behavior and electrical properties of carbon nanotube-Ni nanocomposite films for co-fireable microcircuit electrodes. Thin Solid Films, 2018, 660(AUG.30):754-758. https://doi.org/10.1016/j.tsf.2018.03.080
[6] Fathian Z , Maleki A , Niroumand B . Synthesis and characterization of ceramic nanoparticles reinforced lead-free solder. Ceramics International, 2017, 43(6):5302-5310.
[7] Blinov M I , Shakhov M A , VV Rylko v , et al. Magnetoresistance of (Co_(40)Fe_(40)B_(20))_x(SiO_2)_(100-x) and (Co_(84)Nb_(14)Ta_2)_x(Al_2O_3)_(100-x) nanocomposites below the percolation threshold in pulsed magnetic fields. Journal of magnetism and magnetic materials, 2019, 469(JAN.):155-160. https://doi.org/10.1016/j.jmmm.2018.08.023
[8] Hong S J , Zheng X , Park C W . Enhanced flow boiling heat transfer characteristics of R134a on graphene-Cu nanocomposite coating on copper substrate. International communications in heat and mass transfer, 2019, 108(Nov.):104343.1-104343.7.
[9] Zhang S , Yan L , Gao K , et al. Thermal ratchetting effect of AMB-AlN ceramic substrate: Experiments and calculations. Ceramics International, 2019, 45(12):14669-14674. https://doi.org/10.1016/j.ceramint.2019.04.186
[10] Sasidharanpillai A , Thomas S M , Lee Y , et al. Ultra-low temperature co-fired CaV2O6-glass composite ceramic substrate for microelectronics. Journal of materials science, 2019, 30(8):7637-7644. https://doi.org/10.1007/s10854-019-01079-5
[11] Ryosuke T , Nobuaki T , Yoshiki Y , et al. Post-annealing effects in two-dimensional spin system SrCuO2 sputtered on glass substrate. Journal- Ceramic Society Japan, 2017, 125(5):423-426. https://doi.org/10.2109/jcersj2.16328
[12] Su Y , Zhang W , Lan J , et al. Flexible Reduced Graphene Oxide/Polyacrylonitrile Dielectric Nanocomposite Films for High-Temperature Electronics Applications. ACS Applied Nano Materials, 2020, 3(7):7005-7015. https://doi.org/10.1021/acsanm.0c01328
[13] Baharvandi, H, R, et al. Two-Dimensional Fe Simulation Of Impact Loading On Alumina Matrix Nanocomposite Reinforced By Dyneema (R) Hb25 Laminates. Journal of mechanics, 2017, 33(1):1-11. https://doi.org/10.1017/jmech.2016.26
[14] D M?Ncke, Ehrt R , D Palles, et al. A multi technique study of a new lithium disilicate glass-ceramic spray-coated on ZrO2 substrate for dental restoration. Biomedical glasses, 2017, 3(1):41-55.
[15] Helland A , Kastenholz H , Thidell A , et al. Nanoparticulate materials and regulatory policy in Europe: An analysis of stakeholder perspectives. Journal of Nanoparticle Research, 2018, 8(5):709-719.
[16] Wang R , Lu K Q , Tang Z R , et al. Recent progress in carbon quantum dots: synthesis, properties and applications in photocatalysis. Journal of Materials Chemistry A, 2017, 5(8):3717-3734. https://doi.org/10.1039/C6TA08660H
[17] Shengxue, Yang, Chengbao, et al. Gas sensing in 2D materials.. Applied Physics Reviews, 2017, 4(2):1-34. https://doi.org/10.1063/1.4983310
[18] Nardin C , Winterhalter M , Meier W . Giant Free-Standing ABA Triblock Copolymer Membranes. Langmuir, 2017, 16(20):7708-7712. https://doi.org/10.1021/la000204t
[19] Zhang F , Pi Y , Cui J , et al. Unexpected Selective Photocatalytic Reduction of Nitrite to Nitrogen on Silver-Doped Titanium Dioxide. Journal of Physical Chemistry C, 2017, 111(9):3756-3761. https://doi.org/10.1021/jp067807j
[20] Rzayev, Javid. Molecular Bottlebrushes: New Opportunities in Nanomaterials Fabrication.

Acs Macro Letters, 2017, 1(9):1146–1149. https://doi.org/10.1021/mz300402x

[21] D Zhang, G?Kce B , Barcikowski S . Laser Synthesis and Processing of Colloids: Fundamentals and Applications. Chemical Reviews, 2017, 117(5):3990-4103.

[22] Smith B R , Gambhir S S . Nanomaterials for In Vivo Imaging. Chemical Reviews, 2017, 117(3):901-986.

[23] Mcgillicuddy E , Murray I , Kavanagh S , et al. Silver nanoparticles in the environment: Sources, detection and ecotoxicology. Science of the Total Environment, 2017, 575(jan.1):231-246.

[24] Hildebrandt N , Spillmann C M , Algar W R , et al. Energy Transfer with Semiconductor Quantum Dot Bioconjugates: A Versatile Platform for Biosensing, Energy Harvesting, and Other Developing Applications. Chemical Reviews, 2017, 117(2):536-711.

[25] Li S , Wei W , Liang F , et al. Heavy metal removal using nanoscale zero-valent iron (nZVI): Theory and application. Journal of Hazardous Materials, 2017, 322(Pt A):163-171.

[26] Miller M R , Raftis J B , Langrish J P , et al. Inhaled Nanoparticles Accumulate at Sites of Vascular Disease. ACS Nano, 2017, 11(5):4542-4552. https://doi.org/10.1021/acsnano.6b08551

[27] Ding Y , Kuhlbusch T A , Van T M , et al. Airborne engineered nanomaterials in the workplace-a review of release and worker exposure during nanomaterial production and handling processes.. Journal of Hazardous Materials, 2017, 322(Pt A):17-28.

[28] Noto V D , Piga M , Giffin G A , et al. Influence of Anions on Proton-Conducting Membranes Based on Neutralized Nafion 117, Triethylammonium Methanesulfonate, and Triethylammonium Perfluorobutanesulfonate. 2. Electrical Properties. Journal of Physical Chemistry C, 2017, 116(1):1370-1379. https://doi.org/10.1021/jp204242q

[29] Xu J , Wang Y , Hu S . Nanocomposites of graphene and graphene oxides: Synthesis, molecular functionalization and application in electrochemical sensors and biosensors. A review. Microchimica Acta, 2017, 184(1):1-44. https://doi.org/10.1007/s00604-016-2007-0